IL NUOVO CIMENTO **45 C** (2022) 197
DOI 10.1393/ncc/i2022-22197-1

COMMUNICATIONS: SIF Congress 2021

In silico validation of MCID tool for voxel dosimetry applied to ^{90}Y radioembolization of liver malignancies

A. MILANO([1])([2])(*), A. VERGARA GIL([3]), E. FABRIZI([4]), M. CREMONESI([5]), I. VERONESE([6]), S. GALLO([6]), N. LANCONELLI([7]), R. FACCINI([2]) and M. PACILIO([8])

([1]) *Fondazione Policlinico Universitario "A. Gemelli" IRCCS and UCSC - 00168 Rome, Italy*
([2]) *Department of Physics, Università di Roma "La Sapienza" - 00185 Rome, Italy*
([3]) *CRCT, UMR 1037, Inserm, Université Toulouse III Paul Sabatier - 31062 Toulouse, France*
([4]) *Dipartimento di Scienze di Base ed Applicate per L'ingegneria, Università di Roma "La Sapienza" - 00185 Rome, Italy*
([5]) *Medical Physics Unit, European Institute of Oncology IRCCS - 20141 Milano, Italy*
([6]) *Department of Physics, Università degli Studi di Milano - 20133 Milano, Italy*
([7]) *Department of Physics and Astronomy, Università di Bologna - 40126 Bologna, Italy*
([8]) *Department of Medical Physics, A.O.U. Policlinico Umberto I - 00161 Rome, Italy*

received 31 January 2022

Summary. — The aim of this work is validating the Monte Carlo Internal Dosimetry (MCID) tool for internal dosimetry, which allows personalized treatment planning starting from patient-specific images and direct Monte Carlo (MC) simulations. The absorbed dose for different computational phantoms, calculated with MC and with conventional MIRD methods at both organ and voxel level, were compared, obtaining differences of about 0.3% and within 3%, respectively, whereas differences increased (up to 14%) introducing tissue heterogeneities in phantoms. The absorbed dose of spheres with different radius ($10\,\text{mm} \leq r \leq 30\,\text{mm}$), calculated from MC code and from OLINDA/EXM was also compared, obtaining differences varying in the range 2–9% after correcting for partial volume effects (PVEs) from imaging. This work validated the MCID tool which allows the fast generation of input macros for MC simulations, starting from patient-specific images. It also shows the impact of tissue inhomogeneities on dosimetric results and their relevance for an accurate dosimetric plan.

1. – Introduction

Radioembolization is a clinical therapy for the treatment of primary or secondary hepatic lesions. The technique is based on the administration of ^{90}Y loaded microspheres through the hepatic artery, which is the major blood supplier for liver tumors [1]. The vascular targeting and the short range of β^- particles from ^{90}Y decay make this therapy extremely selective: a high dose can be delivered to the lesions while preserving nearby healthy tissues. An accurate evaluation of the absorbed dose in the regions of interest should be performed in order to optimize and personalize the treatment required. Different dosimetric approaches were developed throughout the years to address this question:

(*) E-mail: alessia.milano03@icatt.it

MIRD at organ level [2], local deposition method [3], Voxel S-Values convolution [4] and Monte Carlo (MC) simulations [5]. The latter are considered the gold standard method, since they take into account both morphological and functional images of the patient. Different MC-based dosimetric tools were developed in the last years but they have not been integrated in the clinical practice yet, mainly because of their high computational times and the lack of validation processes. This work deals with the physical validation of a novel treatment planning system (TPS) named MCID (MC Internal Dosimetry tool), performing Monte Carlo-based voxel dosimetry, applied to ^{90}Y-radioembolization of liver malignancies [6]. The features of the MCID tool allow for the preparation of a personalized simulation, accounting for the specific patient morphology and activity distribution, in a very short time, avoiding manual coding-related difficulties. The impact of possible inhomogeneities on the dosimetric evaluation was also assessed as a secondary aim of the work. A thorough description of the methods, workflow and results of this study can be found in [6].

2. – Materials and methods

For the validation workflow (fig. 1) voxelized phantoms were defined, starting from real patient images. The choice of using phantoms was expressly made in order to set activity ground truth and to easily define different density/activity combinations by properly modifying the phantom. SPECT images (matrix size $128\times128\times120$, pixel size of 0.41 cm) were simulated for each phantom using the SIMIND MC code [7] and they were uploaded into MCID software along a co-registered morphological image (CT). MCID can generate input files for GATE [8] starting from these images and 10^8 primaries were selected for the simulation. Absorbed dose images obtained from the GATE simulation and the ones calculated with other techniques, such as Voxel S-Values convolution using an appropriate ^{90}Y kernel, were compared.

2˙1. *Simulated cases.* – Voxelized phantoms were designed, simulating three clinical cases (Uniform Liver-UL, Spherical Regions-SR and Non-Uniform Liver-NUL) with different activity and density maps. The assigned materials and segmentations are described in [6] and the ICRU atomic composition was always assigned [9]. The UL case has liver with homogeneous density, uniform activity inside the liver and no activity outside of it. This scenario was designed in order to compare the average absorbed dose calculated by the MC-based TPS with the average absorbed dose calculated by the classical AAPM (American Association of Physicists in Medicine) formula [1]. The Spherical Regions (SR) case has homogeneous liver and activity in three spherical regions only (radius 10 mm, 20 mm and 30 mm). We developed this scenario in order to compare the average absorbed dose for each sphere obtained from the GATE output with that obtained from OLINDA/EXM [10] S-factor for ^{90}Y and spheres of soft tissues with unit density. Finally, the Non-uniform Liver (NUL) case can be divided into two subcases: NUL-a, presenting a liver with homogeneous density and activity placed inside both spherical regions and liver with activity concentration ratio of 5:1, respectively; NUL-b, presenting a liver with nonhomogeneous density and activity placed inside the spherical regions (possible tumor lesions) and liver with activity concentration ratio of 5:1, respectively. Higher activity is placed in spherical regions in order to simulate possible lesions which receive higher activity during the procedure.

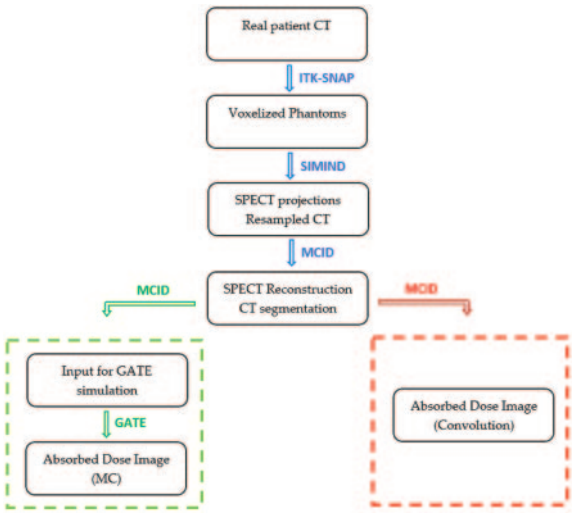

Fig. 1. – Schematic representation of the workflow and software packages used in this study. Figure taken from [6].

3. – Results

Details about the assessment of statistical uncertainties for the obtained results are reported in [6]. All the relative differences (RD) in the following are intended with respect to the GATE absorbed dose value.

For the UL case, the comparison between the mean absorbed dose values to the liver calculated with the MIRD approach at the organ level and direct MC simulation showed a RD of 0.3%. For the SR case, the comparison between average absorbed dose values for each sphere, after the correction for partial volume effects (PVEs), is reported in table I.

For the NUL case, several absorbed dose profiles for each subcase were extracted from different transversal slices. The relative differences of the absorbed dose for each voxel for two selected profiles of NUL-a and NUL-b scenarios are plotted in fig. 2. All the profiles selected for the NUL-a case showed a relative difference within 3% between the two methods. For the NUL-b case, instead, the RDs between the absorbed dose images were up to 14% in the spherical regions, having a different density (1.200 g/cm^3) as compared to the surrounding liver (1.050 g/cm^3).

4. – Discussion

The validation of the MCID platform is demonstrated at both organ (RD = 0.3%) and voxel level (RD within 3%). For the spherical regions case, after the correction for partial volume effects, relative differences were higher (up to 9% for the smallest sphere), possibly due to some differences between the MC codes used for calculating the OLINDA/EXM sphere S-factors and the updated code used in this work, and to possible mismatch in source description. Finally, the presence of inhomogeneities led the differences up to 14%, therefore they should be taken into account in order to realize accurate and personalized results for the patient.

TABLE I. – *Mean absorbed dose values for spheres of different radius (R), calculated from the GATE image (D_{gate}) and from the application of the OLINDA/EXM factors (D_{olinda}). RD is the relative difference between the two values with respect to D_{gate}.*

R (mm)	D_{gate} (Gy)	D_{olinda} (Gy)	RD (%)
30	613	625	−1.92
20	588	604	−2.65
10	517	571	−9.46

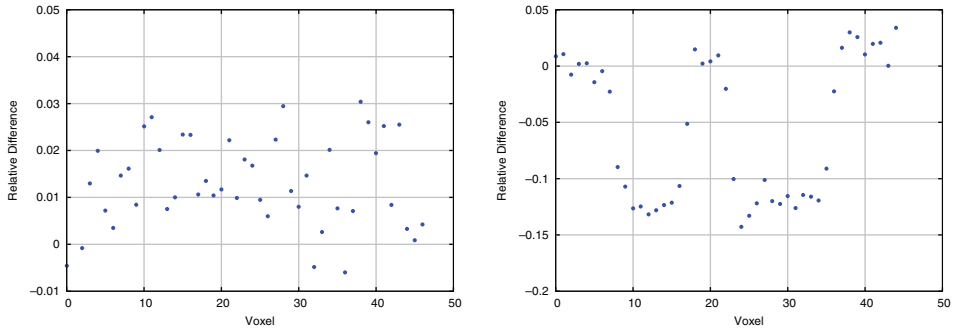

(a) NUL-a (b) NUL-b

Fig. 2. – Relative difference between the absorbed dose profiles extracted from the MIRD and GATE images for the NUL-a case (a) and the NUL-b case (b). The voxels are ordered following the extracted profile. The peaks in (b) correspond to the spherical regions. Figure taken from [6].

5. – Conclusions

The validated MCID platform allows fast implementation of a personalized MC dosimetry and could easily be integrated in the clinical practice. The comparison of absorbed dose values calculated with conventional MIRD approaches and with MC simulations showed good agreement in case of homogeneous and large regions. Relative differences are higher in case of small lesions due to PVEs and in presence of inhomogeneities. The latter should be considered in the dosimetric plan to obtain accurate and optimized results for the patient.

REFERENCES

[1] DEZARN W. A. *et al.*, *Med. Phys.*, **38** (2011) 4824.
[2] GULEC S. A. *et al.*, *J. Nucl. Med.*, **47** (2006) 1209.
[3] PASCIAK A. S. *et al.*, *Front. Oncol.*, **4** (2014) 121.
[4] BOLCH W. E. *et al.*, *J. Nucl. Med.*, **40** (1999) 11S.
[5] PETITGUILLAUME A. *et al.*, *J. Nucl. Med.*, **55** (2014) 51.
[6] MILANO A. *et al.*, *Appl. Sci.*, **11** (2021) 1939.
[7] LJUNGBERG M. *et al.*, *Monte Carlo Calculations in Nuclear Medicine* (CRC Press) 2012, pp. 145–163.
[8] JAN S. *et al.*, *Radiat. Phys. Chem.*, **49** (2004) 4543.
[9] WHITE D. R. *et al.*, *J. ICRU*, **os23** (1989) 20.
[10] STABIN M. G. *et al.*, *J. Nucl. Med.*, **46** (2005) 1023.